

Stabilization of an Unusual Salt Bridge in Ubiquitin by the Extra C-Terminal Domain of the Proteasome-Associated Deubiquitinase UCH37 as a Mechanism of Its Exo Specificity

Marie E. Morrow,[†] Myung-Il Kim,[†] Judith A. Ronau,[†] Michael J. Sheedlo,[†] Rhiannon R. White,[‡] Joseph Chaney,[†] Lake N. Paul,[§] Markus A. Lill,^{||} Katerina Artavanis-Tsakonas,[‡] and Chittaranjan Das^{*,†}

[†]Department of Chemistry, Purdue University, 560 Oval Drive, West Lafayette, Indiana 47907, United States

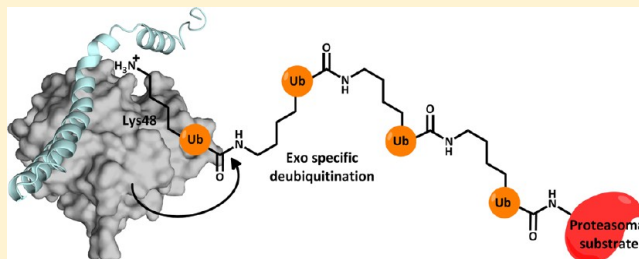
[‡]Division of Cell and Molecular Biology, Imperial College London, Sir Alexander Fleming Building, Imperial College Road, London SW7 2AZ, U.K.

[§]Bindley Biosciences Center, Purdue University, West Lafayette, Indiana 47907, United States

^{||}Department of Medicinal Chemistry and Molecular Pharmacology, Purdue University, 575 Stadium Mall Drive, West Lafayette, Indiana 47907, United States

S Supporting Information

ABSTRACT: Ubiquitination is countered by a group of enzymes collectively called deubiquitinases (DUBs); ~100 of them can be found in the human genome. One of the most interesting aspects of these enzymes is the ability of some members to selectively recognize specific linkage types between ubiquitin in polyubiquitin chains and their endo and exo specificity. The structural basis of exo-specific deubiquitination catalyzed by a DUB is poorly understood. UCH37, a cysteine DUB conserved from fungi to humans, is a proteasome-associated factor that regulates the proteasome by sequentially cleaving polyubiquitin chains from their distal ends, i.e., by exo-specific deubiquitination. In addition to the catalytic domain, the DUB features a functionally uncharacterized UCH37-like domain (ULD), presumed to keep the enzyme in an inhibited state in its proteasome-free form. Herein we report the crystal structure of two constructs of UCH37 from *Trichinella spiralis* in complex with a ubiquitin-based suicide inhibitor, ubiquitin vinyl methyl ester (UbVME). These structures show that the ULD makes direct contact with ubiquitin stabilizing a highly unusual intramolecular salt bridge between Lys48 and Glu51 of ubiquitin, an interaction that would be favored only with the distal ubiquitin but not with the internal ones in a Lys48-linked polyubiquitin chain. An inspection of 39 DUB–ubiquitin structures in the Protein Data Bank reveals the uniqueness of the salt bridge in ubiquitin bound to UCH37, an interaction that disappears when the ULD is deleted, as revealed in the structure of the catalytic domain alone bound to UbVME. The structural data are consistent with previously reported mutational data on the mammalian enzyme, which, together with the fact that the ULD residues that bind to ubiquitin are conserved, points to a similar mechanism behind the exo specificity of the human enzyme. To the best of our knowledge, these data provide the only structural example so far of how the exo specificity of a DUB can be determined by its noncatalytic domain. Thus, our data show that, contrary to its proposed inhibitory role, the ULD actually contributes to substrate recognition and could be a major determinant of the proteasome-associated function of UCH37. Moreover, our structures show that the unproductively oriented catalytic cysteine in the free enzyme is aligned correctly when ubiquitin binds, suggesting a mechanism for ubiquitin selectivity.



The ubiquitin proteasome system (UPS), present in all eukaryotes, is responsible for the majority of controlled degradation and recycling of proteins within the cell.^{1–5} Polyubiquitinated, and to some extent monoubiquitinated, proteins are recognized and degraded by the 26S proteasome, a 2.5 MDa self-compartmentalizing proteolytic complex.^{6–13} It is composed of two major units: the 20S core particle (CP) consisting of 28 subunits and the 19S regulatory particle (RP) containing 19 subunits in yeast. The proteolytic active sites are housed within the luminal chamber of the barrel-shaped CP, capped on both ends by the RP, which contains ubiquitin receptors and enzymes that prepare substrates for degradation.

Entry of substrates into the CP is regulated by the RP, primarily by opening and closing of the substrate translocation channel. Before the substrate is translocated into the narrow channel leading to the lumen of the CP, it is obligatorily deubiquitinated with the help of the RP-resident JAMM metalloprotease Rpn11^{14–16} and unfolded by Rpt subunits that sit within the base subcomplex of the RP.^{7,9,14} However, additional regulation

Received: March 11, 2013

Revised: April 25, 2013

Published: April 25, 2013

is performed by proteasome-associated deubiquitinating enzymes, whose underlying mechanism is still poorly understood.^{7,17}

Attachment of ubiquitin to a lysine residue(s) on target proteins is catalyzed by the sequential action of three enzymatic systems: E1 (ubiquitin-activating), E2 (ubiquitin-conjugating), and E3 (ubiquitin-ligating) enzymes.^{18,19} Usually, ubiquitination of a target protein results in the attachment of a polyubiquitin chain in which successive ubiquitin moieties are attached to one of the seven lysines, or the N-terminal amino group of the preceding monomer, to generate a homopolymeric structure.^{18,20} Polyubiquitin chains of a distinct topology are thus generated depending on which amino group of ubiquitin is used for chain extension (lysines 6, 11, 27, 29, 33, 48, and 63 or the amino group of Met1). A polyubiquitin chain of a specific topology is meant for a specific type of functional outcome.^{20–25} For example, a Lys48 (K48)-linked chain usually serves as the signal for proteasomal degradation, whereas K63 chains signal other types of functions such as endocytosis, DNA repair, and NF- κ B signaling.^{24,26}

Ubiquitination works as a reversible post-translational modification, like phosphorylation. Deubiquitinating enzymes, or DUBs, can hydrolytically remove ubiquitin from protein adducts, thereby opposing the action of ubiquitin conjugating machinery.^{27–33} Consequently, DUBs have been found to play important regulatory roles in numerous ubiquitin-dependent cellular processes.^{32–35} In mechanistic terms, these enzymes can be categorized into two main groups: cysteine proteases and zinc metalloproteases. The zinc metalloproteases consist of only one family, the JAB1/MPN/MOV34 metalloenzymes (JAMMs). The cysteine proteases are further broken down into four families based on the structure of their catalytic domain: ubiquitin carboxyl-terminal hydrolases (UCHs), ubiquitin-specific proteases (USPs), ovarian tumor proteases (OTUs), and Machado-Josephin domain proteases (MJDs).³²

UCH37 (also known as UCHL5) is a 37 kDa DUB of the UCH family and is one of the two proteasome-associated DUBs, the other being USP14 (Ubp6 in yeast), known to regulate protein degradation by the mammalian proteasome.^{36–40} These associated DUBs, along with Rpn11, a constitutive member of the RP, conduct deubiquitination at the proteasome. However, the activities of the three enzymes are distinct. Rpn11 is responsible for en-bloc removal of polyubiquitin chains prior to (or concurrent with) unfolding and translocation of the substrate into the CP, an activity that appears to be coupled to substrate degradation.^{15–17} USP14 and UCH37 on the other hand are known to have chain-trimming functions.^{17,37,41} The importance of these associated DUBs to proteasome function was revealed through pharmacological inhibition of these enzymes. A small-molecule inhibitor of USP14 appears to accelerate proteasomal degradation of certain substrates, whereas UCH37 inhibition can stall proteolysis, consistent with distinct functional roles played by the two enzymes.^{42–44}

UCH37 was first identified as the PA700 isopeptidase, the cysteine DUB tightly associated with the RP, also known as PA700.^{38,45,46} Like other UCH family members, it contains a conserved catalytic triad of a cysteine, a histidine, and an aspartate. UCH37 has a canonical UCH domain that is 45% similar to UCHL1 and 49% similar to UCHL3, its single-domain family members.^{47–50} It also has an additional C-terminal tail domain responsible for its interaction with the Rpn13 subunit of the RP.^{51–54} Proteasome-bound UCH37 is

thought to behave as an “editor”, relieving poorly ubiquitinated substrates from degradation by sequentially dismantling their K48-linked polyubiquitin chains from the very distal end, removing one ubiquitin at a time.^{37,38,45} Such a type of chain disassembling activity can be termed as an exo cleavage activity in contrast to the endo activity, which leads to dismantling of chains by cleavage between internal ubiquitins. Although it has respectable UbAMC (ubiquitin aminomethylcoumarin) hydrolysis activity in its unbound form, UCH37 has been shown to require association with the proteasome to cleave diubiquitin (and polyubiquitin) chains.³⁷ Additionally, its UbAMC hydrolysis activity is enhanced upon binding with Rpn13.^{37,54} Interestingly, UCH37 also associates in the nucleus with the human Ino80 chromatin remodeling complex, where it is held in an inactive state compared to the free enzyme.⁵⁵ It thus serves as an example of a DUB whose catalytic activity is both positively and negatively regulated by binding to specific protein partners, making it an attractive target for structural studies. Crystal structures have been determined for both the catalytic domain and full-length human UCH37,^{56–58} however, the mechanism of its catalytic regulation upon binding to associated protein factors is not known. Any mechanistic understanding of its regulation must require structural information about UCH37 and its catalytic domain bound to ubiquitin, which has yet to be reported.

TsUCH37 is a recently characterized lower-organism homologue of UCH37 from *Trichinella spiralis* (Ts), an infectious helminth found nearly worldwide. TsUCH37 was identified by White et al. by incubation of the whole-cell lysate of Ts larvae with the HA-UbVME probe (HA, the hemagglutinin epitope, fused with the N-terminus of ubiquitin vinyl methyl ester), an epitope-tagged irreversible inhibitor of cysteine DUBs.⁵⁹ Its structural and functional homology with human UCH37 was then confirmed by sequence analysis, co-immunoprecipitation with proteasomal subunits, and UbAMC hydrolysis assays. TsUCH37 is 45% identical to its human homologue and was shown to pull down TsADRM1, the corresponding Rpn13 homologue, by co-immunoprecipitation.⁵⁹ The sequence and functional conservation between the Ts and human enzymes implies a similar chain-editing role of the former at the proteasome. To understand the mechanisms associated with UCH37, we have crystallized two constructs of TsUCH37 bound to ubiquitin vinyl methyl ester. The structures illuminate the mode of ubiquitin recognition in the enzyme by revealing binding interactions with the catalytic domain, which are conserved among UCH enzymes, and interactions unique to UCH37, notably ubiquitin binding by the ULD, providing further explanation of the proteasome-associated exo-specific deubiquitination activity of the DUB.

MATERIALS AND METHODS

Cloning, Expression, and Purification. *TsUCH37^{cat}*. *TsUCH37^{cat}* (residues 1–226) was subcloned from the full-length construct (residues 1–309) in pET28a(+) into pGEX-6P-1 (GE Biosciences) using BamHI and XhoI restriction sites. The protein was expressed in *Escherichia coli* Rosetta cells (Novagen) grown at 37 °C in LB medium containing 100 μ g/L ampicillin to an OD₆₀₀ of 1.0 and then induced with 0.5 mM isopropyl β -D-thiogalactoside (IPTG) at 18 °C for 16 h. Harvested cells were resuspended in lysis buffer (1 \times phosphate buffered saline and 400 mM KCl) and lysed with a French press. The lysate was then purified on a glutathione S-transferase (GST) column (GE Biosciences) followed by

cleavage of the GST tag by PreScission Protease (GE Biosciences) per the manufacturer's instructions. It was further purified by size exclusion chromatography on a Superdex 75 column (GE Biosciences). Intein-fused ubiquitin₁₋₇₅ in pTXB1 was expressed in *E. coli* Rosetta cells and purified on chitin beads (New England Biosciences). Ubiquitin vinyl methyl ester (UbVME) was synthesized by overnight incubation of Ub₁₋₇₅-MESNa (MESNa, sodium mercaptoethanesulfonate) with glycine vinyl methyl ester and then purified on a MonoS cation exchange column (GE Biosciences). Glycine vinyl methyl ester was synthesized by a modified, previously published procedure.⁶⁰ TsUCH37^{cat} was reacted with UbVME for 4 h, followed by purification on a MonoQ anion exchange column (GE Biosciences) to separate any unreacted TsUCH37^{cat}. Selenomethionine TsUCH37^{cat} protein (SeMet TsUCH37^{cat}) was grown in M9 minimal medium supplemented with selenomethionine, reacted with UbVME, and purified as described above.

TsUCH37^{ΔC46}. TsUCH37^{FL} was subcloned previously into pET28a(+) with an N-terminally fused His tag (Novagen). TsUCH37^{FL} was expressed in *E. coli* Rosetta cells, grown at 37 °C in LB medium containing 10 μg/L kanamycin to an OD₆₀₀ of 0.8, and then induced with 0.5 mM IPTG at 18 °C for 16 h. Harvested cells were resuspended in lysis buffer [50 mM Tris-HCl (pH 7.6), 200 mM NaCl, and 3 mM β-mercaptoethanol] and lysed with a French press. His-tagged TsUCH37^{FL} was purified by immobilized metal affinity chromatography (IMAC) and eluted with lysis buffer including 500 mM imidazole. Eluted proteins were further purified by size exclusion chromatography (SEC) on a Superdex 75 column (GE Biosciences) in 50 mM HEPES (pH 7.6) and 3 mM dithiothreitol (DTT). SDS-PAGE on the fractions indicated a cleavage of the full-length protein, so the construct described is actually a proteolytic cleavage product of the full-length protein. The crystal structure (described below) lacks density for the last 46 amino acids from the C-terminus; therefore, this construct will hereafter be described as TsUCH37^{ΔC46}. Fractions containing the target protein were pooled, concentrated, and reacted with UbVME. UbVME was synthesized and reacted with purified TsUCH37^{ΔC46} as was done with TsUCH37^{cat}. To separate unreacted TsUCH37^{ΔC46}, the complex was further purified by SEC on a Superdex 75 column (GE Biosciences).

Crystallization and Structure Determination. **TsUCH37^{cat}-UbVME Complex.** The TsUCH37^{cat}-UbVME complex was concentrated to 3 mg/mL in 50 mM Tris (pH 7.6), 200 mM NaCl, and 1 mM DTT. Crystals were grown in 2 days at room temperature by hanging drop vapor diffusion in 3 M ammonium sulfate and 0.1 M bicine (pH 9.0) with 2 mM L-glutathione (mixture of oxidized and reduced) additive. Crystals were cryoprotected in 2.5 M sodium malonate and flash-frozen in liquid nitrogen.⁶¹ Diffraction data were collected on a Mar300 CCD detector (Mar USA) at the 23-ID-B beamline at Argonne National Laboratory (Argonne, IL). Data up to 1.7 Å were collected on SeMet TsUCH37^{cat}-UbVME crystals at the selenium peak (0.979 Å) for SAD (single-wavelength anomalous dispersion) phasing. Data were processed with HKL2000.⁶²

The initial model was obtained by Se-SAD phasing in the Phenix AutoSol wizard.⁶³ Its sequence was built in using the Phenix AutoBuild wizard, as well as manual model building in Coot.^{63,64} Structural refinement was conducted in Phenix using TLS refinement (with the entire asymmetric unit taken as one TLS group), as well as optimized weighting for stereochemical

restraints.⁶³ The data were run through Phenix Xtriage, which confirmed the chosen space group, C2, and did not detect evidence of crystal twinning.⁶³ The completeness of the crystallographic data for the TsUCH37^{cat}-UbVME complex was less than ideal (see Table 2); however, this did not hinder the determination of the structure or the generation of the structural model presented herein and can be ascribed to poor completeness in the highest-resolution shells.

TsUCH37^{ΔC46}-UbVME Complex. The TsUCH37^{ΔC46}-UbVME complex was concentrated to 5 mg/mL in 50 mM HEPES (pH 7.6) and 2 mM DTT. Crystals were grown in 60 days at room temperature in 0.2 M ammonium chloride (pH 5.8) and 18% PEG3350. Crystals were cryoprotected in ethylene glycol and flash-frozen in liquid nitrogen. Diffraction data were collected on a Mar300 CCD detector (Mar USA) at the 23-ID-B beamline at Argonne National Laboratory. Data up to 2.0 Å were collected on TsUCH37^{ΔC46}-UbVME crystals at 1.033 Å. Data were processed with HKL2000.⁶²

The initial model was obtained by molecular replacement using the Phenix AutoMR wizard, with a monomer of the TsUCH37^{cat}-UbVME complex as the search model.⁶³ Manual model building was conducted in Coot, and structural refinement was conducted initially in Refmac using TLS refinement and then using simulated annealing and individual B factor refinement in Phenix.^{63,64} The data were run through Phenix Xtriage, which confirmed the chosen space group, R3, and did not detect any evidence of crystal twinning.⁶³

UbAMC Hydrolysis Assay. TsUCH37^{cat} was diluted in reaction buffer [50 mM Tris (pH 7.6), 0.5 mM EDTA, 0.1% bovine serum albumin, and 5 mM DTT] to a final reaction concentration of 7 nM and preincubated at 30 °C for 5 min prior to the addition of the UbAMC substrate (Boston Biochem). UbAMC cleavage was measured on a Tecan (Männedorf, Switzerland) fluorescence plate reader with 380 nm excitation and 465 nm emission wavelengths at 30 °C. Data were fit to Michaelis-Menten kinetics in SigmaPlot (Systat Software, San Jose, CA).

Analytical Ultracentrifugation. Sedimentation velocity experiments were conducted with the Beckman-Coulter XLA analytical ultracentrifuge. The sample was extensively dialyzed against 50 mM Tris-HCl, 200 mM NaCl, and 1 mM DTT (pH 7.4). The TsUCH37^{cat} and TsUCH37^{cat}-UbVME complex concentration ranged from 10 to 32 μM. The samples were centrifuged at 50000 rpm using a two-sector 1.2 cm path-length carbon-filled Epon centerpiece. The experiments were conducted on an An-50 Ti rotor at 20 °C. The density and relative viscosity of the buffers were calculated using SEDNTERP version 1.09 (<http://www.rasmb.bbri.org/rasmb/windows/sednterp-phil0>): 1.0079 g/mL and 0.01036 P, respectively. The partial specific volume (v_{bar}) of the protein was also calculated from the protein sequence using SEDNTERP (0.7340 mL/g for TsUCH37^{cat} and 0.7317 mL/g for the TsUCH37^{cat}-UbVME complex). The samples were monitored at 280 nm with a 4 min delay and 150 scans. The c(s) distributions were analyzed using SEDFIT version 13.0b.⁶⁵

Molecular Dynamics Simulations. A model of full-length TsUCH37 was generated by the SwissModel homology modeling server using the structure of the full-length human protein as a template.⁶⁶ Missing ULD residues produced by the model were appended to the TsUCH37^{ΔC46}-UbVME structure in Coot, and a single round of refinement was conducted in Phenix, to produce a final model hereafter termed "the system".^{63,64} The system was solvated in a box of TIP3P

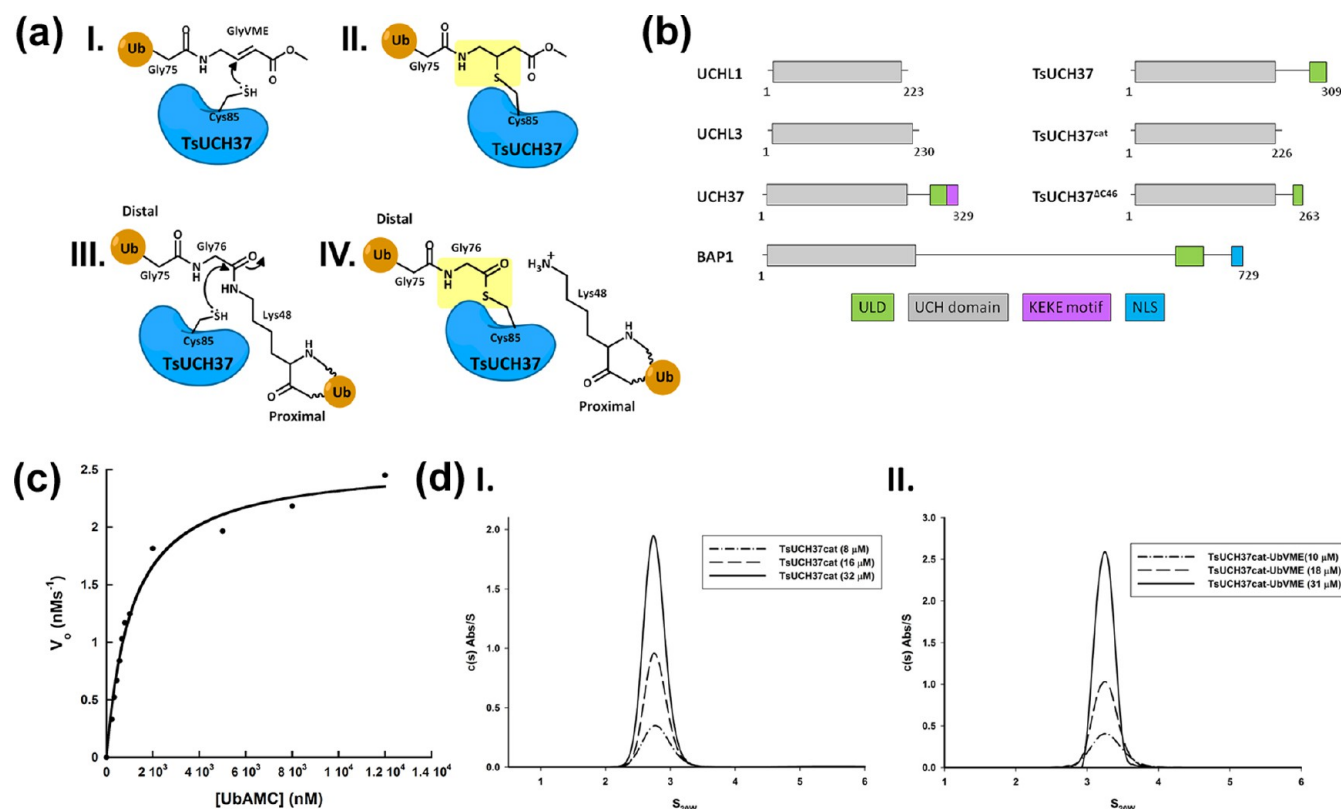


Figure 1. (a) Schematic structures representing inhibition of UCH37 by UbVME (I and II). Definition of proximal and distal ubiquitin in a diubiquitin substrate (III). Schematic structure of the acyl-enzyme intermediate formed during deubiquitination catalyzed by a cysteine DUB (IV). The UbVME adduct (II) mimics the acyl-enzyme intermediate (IV), as shown in yellow. (b) Domain diagrams of TsUCH37 constructs compared to other UCH family members with UCH domains boxed in gray and additional domains boxed and labeled as shown. (c) Kinetic assay of UbAMC hydrolysis by TsUCH37^{cat}. (d) Analytical ultracentrifugation profiles of TsUCH37^{cat} (left) and the TsUCH37^{cat}-UbVME complex (right), indicating that both are monomeric in solution.

water with the minimal distance between any solute atom and the boundary of the box set to 10 Å. The system was neutralized with 15 Na⁺ ions, which were automatically positioned by the tleap program. Molecular dynamics (MD) simulations were performed using Amber 10 with Amber force field ff03.⁶⁷ Periodic boundary conditions were applied, and the full electrostatic energy was calculated using the particle mesh Ewald (PME) method.⁶⁸ The simulation consisted of three sequential steps: energy minimization for 5000 steps (2500 steps of steepest-descent followed by 2500 steps of conjugate gradient minimization), equilibration for 100 ps of solvent with the protein restraint with a force constant of 5 kcal mol⁻¹ Å⁻¹, and a final MD simulation for 2 ns. All simulations were conducted at 300 K with a constant volume. A time step of 2 fs was used, and the SHAKE algorithm was applied to constrain the bonds involving hydrogen atoms.⁶⁹

RESULTS

TsUCH37, like its mammalian counterpart, contains a catalytic UCH domain, and an additional polypeptide chain following it called the C-terminal tail comprising the conserved UCH37-like domain (ULD) followed by a putative KEKE motif (Figure 1b).^{37,51,70,71} The ULD in human UCH37 is thought to have an inhibitory role, presumably by folding onto the catalytic domain thereby occluding ubiquitin binding.³⁷ However, how ubiquitin binds to UCH37 has not been structurally characterized. To gain insight into how ubiquitin is recognized by TsUCH37, we aimed to crystallize both the catalytic domain of TsUCH37

bound to ubiquitin vinyl methyl ester (UbVME) (the TsUCH37^{cat}-UbVME complex) and the UbVME complex of the full-length protein. UbVME is a suicide substrate of cysteine DUBs, which react with the former via nucleophilic attack of the catalytic cysteine at the vinyl group of the VME moiety, resulting in an irreversible modification whereby a covalent bond is formed between the catalytic cysteine and the VME portion of the inhibitor (Figure 1a).^{36,48,60} This covalent adduct is thought to mimic the acyl-enzyme intermediate formed during deubiquitination reactions catalyzed by the DUB (II and IV in Figure 1a). If diubiquitin is used as the substrate, the distal ubiquitin moiety is the acyl component of the acyl-enzyme intermediate, with the proximal ubiquitin acting as the leaving group during isopeptide bond hydrolysis (in diubiquitin, a lysine residue of one ubiquitin, called the proximal ubiquitin, is linked via an isopeptide bond to the C-terminal carboxylate group of another ubiquitin, called the distal ubiquitin) (III in Figure 1a).

The TsUCH37^{cat}-UbVME complex crystallized in the C2 space group with two molecules of the complex in the asymmetric unit. Our attempts to crystallize the full-length version, however, were met with limited success, the full-length protein being susceptible to proteolysis as indicated by at least two closely migrating bands in an SDS-PAGE gel (data not shown). While attempting to purify the full-length construct, we managed to retrieve a truncated version of the protein lacking 46 amino acids from the C-terminal end of the protein (see Materials and Methods). This truncated protein was

purified by Ni affinity chromatography and reacted with UbVME, and the complex was purified using ion-exchange chromatography. This complex, hereafter termed the TsUCH37^{ΔC46}–UbVME complex (TsUCH37 missing the last 46 residues), crystallized in the R3 space group with one complex in the asymmetric unit.

The catalytic activity of TsUCH37^{cat} was measured with a UbAMC hydrolysis assay (Figure 1c), which yielded Michaelis–Menten parameters as shown in Table 1. Compared

Table 1. Kinetic Parameters for TsUCH37^{cat}

enzyme	K_M (nM)	k_{cat} (s ^{−1})	k_{cat}/K_M (×10 ⁵ M ^{−1} s ^{−1})
TsUCH37 ^{cat}	1085	0.37	3.4
UCH37N240 ^a	21493	34	16
UHL3 ^a	77.1	19	2414
UHL1 ^a	47.0	0.03	7.4

^aKinetic parameters previously determined, from ref 75.

to the catalytic domain of human UCH37, TsUCH37^{cat} has an approximately 20-fold lower K_M , indicating a higher affinity for this substrate compared to that of the human protein, but a 100-fold lower k_{cat} , a substantially lower turnover number. Consequently, TsUCH37^{cat} is nearly 5-fold less efficient than the UCH domain of human UCH37.

Crystals of the TsUCH37^{cat}–UbVME complex diffracted to 1.7 Å. The structure was determined by single-wavelength anomalous dispersion (SAD) using anomalous scattering from selenium (TsUCH37^{cat} was labeled with selenium). Manual model building using Coot, followed by multiple rounds of refinement using Phenix, produced a final model with an R factor of 17.4% and an R_{free} of 21% (see Table 2 for crystallographic and refinement parameters).^{63,64} The final refined model corresponding to the asymmetric unit consists of two copies of the TsUCH37^{cat}–UbVME complex, composed of TsUCH37^{cat}, residues 1–226, covalently connected via a thioether bond linking the catalytic cysteine with the VME group of UbVME (residues 1–75 of ubiquitin attached to GlyVME as the 76th residue, which is modeled as methyl 4-amino butanoate). The refined model was of high stereochemical quality, with <0.2% of residues in the disallowed region of the Ramachandran plot and scoring in the upper 98% according to Molprobit evaluation.⁷² The structure of the TsUCH37^{ΔC46}–UbVME complex (2.0 Å resolution) was determined by molecular replacement using the TsUCH37^{cat}–UbVME structure as the search model (Table 2). The final refined model with good stereochemical quality (<0.2% of residues in the disallowed region of the Ramachandran plot and Molprobit score of 63%) has amino acids 5–263 of the protein and one UbVME linked via a thioether bond to the catalytic cysteine. The structures of the UCH domain in the two constructs are very similar, except for two loop regions (see below), with $C\alpha$ root-mean-square deviations (rmsds) of 0.32 Å between the two (the loop regions were excluded from the calculation of the rmsd). When discussing the structure of the UCH domain alone or its interaction with UbVME, we will therefore use the structure of the TsUCH37^{cat}–UbVME complex because its resolution is higher while specifically mentioning any structural feature that is different in the UCH domain of TsUCH37^{ΔC46}–UbVME complex.

Initial analysis of the structure revealed that the two copies in the asymmetric unit of TsUCH37^{cat}–UbVME crystals are

Table 2. Crystallographic and Refinement Statistics^a

	SeMet TsUCH37 ^{cat} –UbVME	TsUCH37 ^{ΔC46} –UbVME
Data Collection		
space group	C121	R3
cell dimensions		
a, b, c (Å)	171.2, 55.8, 73.9	147.4, 147.4, 40.5
α, β, γ (deg)	90, 113.4, 90	90, 90, 120
wavelength (Å)	0.979	1.033
resolution (Å)	50.00–1.70 (1.73–1.70)	50–2.0 (2.03–2.00)
R_{sym} or R_{merge} ^b (%)	8.7 (50.0)	8.5 (83.8)
$I/\sigma I$	15.9 (3.0)	4.9 (4.1)
completeness (%)	88.5 (42.0)	100.0 (100.0)
redundancy	6.8 (3.5)	5.8 (5.7)
Refinement		
resolution (Å)	27.9–1.7	38.6–2.0
no. of unique reflections	62326/3126	22270/2002
R_{work} ^c / R_{free} ^d	17.4/21.1	19.3/24.0
no. of atoms		
protein ^e	4650	2428
ligand	24	8
water	437	100
average B factor (Å ²)		
protein	36.2	43.4
ligand	36.5	32.4
water	44.0	44.3
rmsd		
bond lengths (Å)	0.013	0.009
bond angles (deg)	1.48	1.07
Ramachandran plot (%)		
favored	98.1	97.7
allowed	1.6	1.0
outliers	0.4	1.3

^aNumbers in parentheses refer to data in the highest-resolution shell. ^b $R_{merge} = \sum |I_h - \langle I_h \rangle| / \sum I_h$, where I_h is the observed intensity and $\langle I_h \rangle$ is the average intensity. ^c $R_{work} = \sum ||F_{obs}| - k|F_{calc}|| / \sum |F_{obs}|$. ^d R_{free} is the same as R_{obs} for a selected subset (5 and 9%) of the reflections that was not included in prior refinement calculations. ^eOrdered residues: Pro3–Gly141 and Lys153–Asp224 in chain C and Pro3–Gly141 and Gln152–Gln225 in chain A of the SeMet TsUCH37^{cat}–UbVME structure and Gly4–Lys57, Thr72–Gly141, and Glu157–Ala263 of the TsUCH37^{ΔC46}–UbVME structure.

linked by a disulfide bond between Cys71 of the two TsUCH37^{cat} chains (Figure 2a). It is possible that the disulfide bond forms because the protein exists as a dimer in solution, bringing the cysteines into proximity of each other, or is a result of crystallographic packing. To determine if this disulfide is a crystallographic artifact or a biologically relevant association, we determined the oligomerization state of complexed and uncomplexed (apo) TsUCH37^{cat} by sedimentation velocity analytical ultracentrifugation (AUC). We found that both the complex and the apo protein exist as monomers in solution with sedimentation coefficients ($S_{20,w}$) of 3.3 and 2.8, respectively (Figure 1d), indicating that this disulfide is likely a result of crystal packing. TsUCH37 is expected to be predominantly localized to the cytosol, a reducing environment, and therefore should not rely on disulfide-mediated dimerization for catalytic activity. Moreover, the observation that the

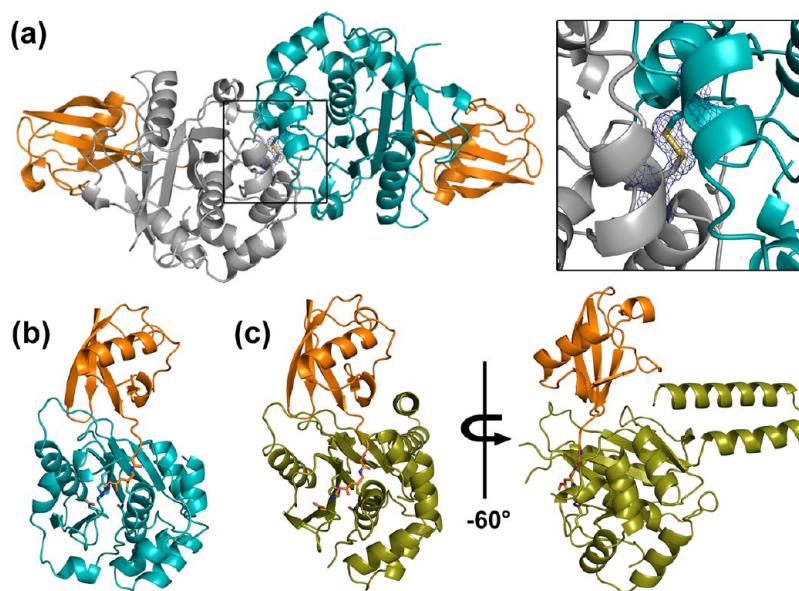


Figure 2. Crystal structures of TsUCH37 constructs bound to UbVME. (a) Dimeric structure of TsUCH37^{cat} bound to UbVME (orange) in crystals. Monomers are colored teal (chain A) and gray (chain C). The inset shows the disulfide bridge that links the two subunits via Cys71. The electron density is rendered from the $2F_o - F_c$ map contoured at 1σ . (b) Monomer of the TsUCH37^{cat}-UbVME structure. (c) Structure of the TsUCH37^{ΔC46}-UbVME complex, with TsUCH37^{ΔC46} colored olive and UbVME orange.

TsUCH37^{ΔC46}-UbVME complex is a monomer in the asymmetric unit and that the segment of residues 57–71, which is used as a part of the dimer interface in the crystals of the TsUCH37^{cat}-UbVME complex, is disordered in the TsUCH37^{ΔC46}-UbVME structure (Figures 2 and 3) supports

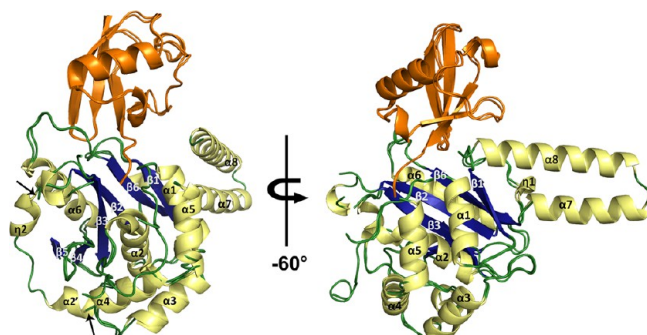


Figure 3. Secondary structures of TsUCH37 constructs. TsUCH37^{ΔC46}-UbVME and TsUCH37^{cat}-UbVME complexes are superposed with α -helices and 3_{10} -helices colored pale yellow, β -sheets blue, loops green, and UbVME orange. Arrows indicate where the TsUCH37^{ΔC46}-UbVME structure lacks density, compared to the TsUCH37^{cat}-UbVME structure, from residue 57 to 71.

the notion that the dimer observed in the TsUCH37^{cat}-UbVME structure is a crystallographic dimer and may not exist in solution. The two copies of the complex in the dimer observed in the crystals of the TsUCH37^{cat}-UbVME complex have very similar structures with an rmsd of 0.39 Å between C α atoms. We will therefore focus on one of them in discussions presented below.

Overall Structure of the UCH Domain of TsUCH37.

The overall structure of the TsUCH37 catalytic domain is similar to that of other structurally characterized UCH enzymes.^{49,50,73} It has the classical $\alpha\beta\alpha$ fold, in which a central six-stranded β -sheet is surrounded by six α -helices, five on one side ($\alpha 1$ – $\alpha 5$) and one on the other ($\alpha 6$) (Figure 3). The

overall architecture of TsUCH37^{cat} can be seen as bilobal, with one of the lobes comprising helices $\alpha 1$ – $\alpha 5$ and the other comprising the β -sheets and helix $\alpha 6$. The active site is located at the interface of the two lobes, with Cys85 from helix $\alpha 2$ in one lobe and His161 from $\beta 3$ in the other forming the catalytic Cys-His pair. An adjacent loop provides the third member of the triad, Asp176. Most of the secondary structural elements seen in TsUCH37^{cat} are conserved in UCHL1 and UCHL3, with the only noticeable difference being the conformation of a segment following $\beta 2$, residues 57–71. This segment is a helix in UCHL1 and UCHL3 and is in somewhat of an extended looplike conformation in human UCH37 (hUCH37) but is fairly ordered; in the structure of the various constructs of human UCH37 determined so far, this loop has been found to be in a similar conformation regardless of crystallographic packing (Figure S1 of the Supporting Information).^{56–58,74} In contrast, this segment appears to be flexible in TsUCH37 and is visualized only in the TsUCH37^{cat}-UbVME structure, in which it forms the dimer interface between the two subunits in the asymmetric unit. In the TsUCH37^{ΔC46}-UbVME complex, a crystallographic monomer, this loop is disordered (Figure 3). Although the possibility that its binding can influence the loop dynamics cannot be ruled out, it is unlikely that UbVME has anything to do with the dynamic behavior of the loop because it does not bind to it. We therefore propose that the loop is intrinsically flexible in TsUCH37 but can become ordered under certain circumstances, such as under the constraints of crystallographic packing.

It is possible that the corresponding loop segment in hUCH37 is somewhat dynamic as well, but it appears to be significantly more flexible in TsUCH37. The significance of this difference in dynamics between the two proteins is not clear at the moment. Intriguingly, the loop's dynamic behavior appears to have an effect on the conformation of a tryptophan residue (Trp55) adjacent to the active site (Figure S2 of the Supporting Information). This tryptophan is conserved among *Schizosaccharomyces pombe* (Sp), Ts, and human UCH37 (Figure S3

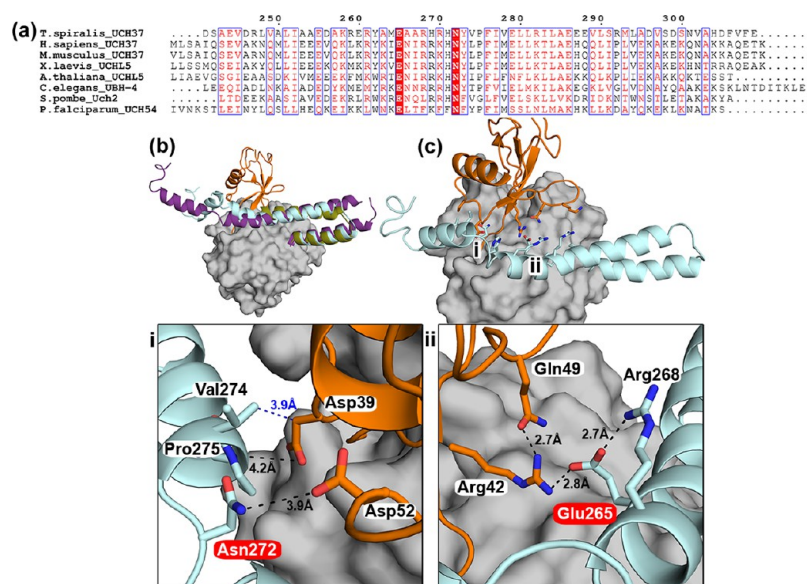


Figure 4. ULD–ubiquitin interactions. (a) Sequence alignment of the ULD of UCH37 highlighting conserved residues in UCH37 homologues. Glu265 and Asn272 (according to *Ts* numbering) are absolutely conserved (highlighted in red). (b) Superposition of the *Ts*UCH37 Δ C46–UbVME complex (ULD colored olive and UbVME orange), human UCH37 (ULD colored purple, PDB entry 3IHR), and *Ts*UCH37 with the entire ULD modeled (cyan) based on the structure of the ULD in human UCH37. The model was generated using SwissModel and MD simulation (please see Materials and Methods). This model is taken from a snapshot collected at 1.3 ns during a 2 ns MD simulation run. (c) Structure of the *Ts*UCH37–ubiquitin complex with the entire ULD modeled as shown in panel b, showing that the conserved residues of the ULD could make additional contacts with ubiquitin. The regions marked i and ii are expanded in the panels below. The UCH domain is colored gray.

of the Supporting Information). In the *Ts*UCH37 Δ C46–UbVME complex, Trp55 makes contact with the OMe group of the suicide inhibitor, which in the actual substrate (a ubiquitinated protein or the diubiquitin motif of a polyubiquitin chain) would be replaced by the hydrocarbon portion of the isopeptide-linked lysine side chain (Figure 1a). The same residue in the *Ts*UCH37 Δ C46–UbVME complex shows a different orientation with respect to the OMe group and appears to have adopted a more open position for interaction with the isopeptide unit (Figure S2 of the Supporting Information). Therefore, Trp55 not only may provide important contacts with the isopeptide link to hold it in place near the active site but also may confer a certain plasticity to the active site of UCH37, which may be useful for an induced-fit type of engagement with the substrate.

As stated before, in the *Ts*UCH37 Δ C46–UbVME structure, we are able to visualize 40 additional amino acids after the UCH domain, the first 41 amino acids (residues 223–263) of the ULD in *Ts*UCH37. The polypeptide chain, after emerging from the C-terminus of the UCH domain, adopts a helical structure of six turns (α 7), takes a U-turn, and then continues as a helix (α 8). α 7 and α 8 are arranged as a helix–turn–helix motif with a number of interhelical contacts, and this motif adopts a similar orientation with respect to the UCH domain as observed in hUCH37 (Figures 3 and 4b).⁵⁷ The only difference in this motif between *Ts*UCH37 and hUCH37 is that it is somewhat shorter in the former. The ULD in *Ts*UCH37 appears to have a proteolytically susceptible region after Ala263, perhaps immediately following it, producing the C-terminal truncation we are observing here. When we model the missing part of the ULD, using the structure of hUCH37 as a template (see Materials and Methods), it is apparent that α 8 could have continued on after the cleavage site (Figure 4b) almost as a long helix all the way up to residue 285, except for an interruption at Arg268 where four successive residues,

including the arginine, adopt nonhelical dihedral angles producing a kink (a kink featuring equivalent residues is also seen in the template structure). As expected from the hUCH37 structure, the model shows that after the interruption, the helix would terminate at or near amino acid 285 (Figure 4), where the polypeptide chain reverses its direction as a turn segment that appears to cap the C-terminus of the helix. The putative KEKE motif was not modeled because it is absent in the template structure. Interestingly, the structure of the *Ts*UCH37 Δ C46–UbVME complex reveals side chains from α 8 making contact with ubiquitin, specifically with its Lys48 residue, an interaction that may explain the distal end specificity displayed by UCH37 (discussed in more detail below). Also, the side chains from the modeled part of the ULD, missing in our structure, appear to present themselves for additional contacts with ubiquitin. Indeed, the two most conserved residues in the ULD, Glu265 and Asn272, are facing ubiquitin and lie within contact distances (Figure 4c). Thus, it is possible that they may actually bind to ubiquitin. Alternatively, in contrast to what is predicted by the model, these residues may be used for making contact with Rpn13, explaining why they are conserved.

Active-Site Geometry. The catalytic triad in this cysteine protease assumes a canonical arrangement in the ubiquitin-bound complex. The distance between the catalytic cysteine and histidine is 3.9 Å ($N\delta$ – $S\gamma$ distance) in both structures, and that between the histidine and aspartate is 2.8 Å ($N\epsilon$ – $O\delta$) in the *Ts*UCH37 Δ C46–UbVME complex and 2.9 Å in the *Ts*UCH37 Δ C46–UbVME complex. The distance between the C ϵ H group of the catalytic histidine and the side chain carbonyl oxygen of the oxyanion stabilizing glutamine (Gln79) is 3.3 Å in the *Ts*UCH37 Δ C46–UbVME complex and 3.1 Å in the *Ts*UCH37 Δ C46–UbVME complex, suggesting a significant CH \cdots O interaction between them, an interaction seen in other cysteine proteases as well.⁷⁵ We were unable to crystallize

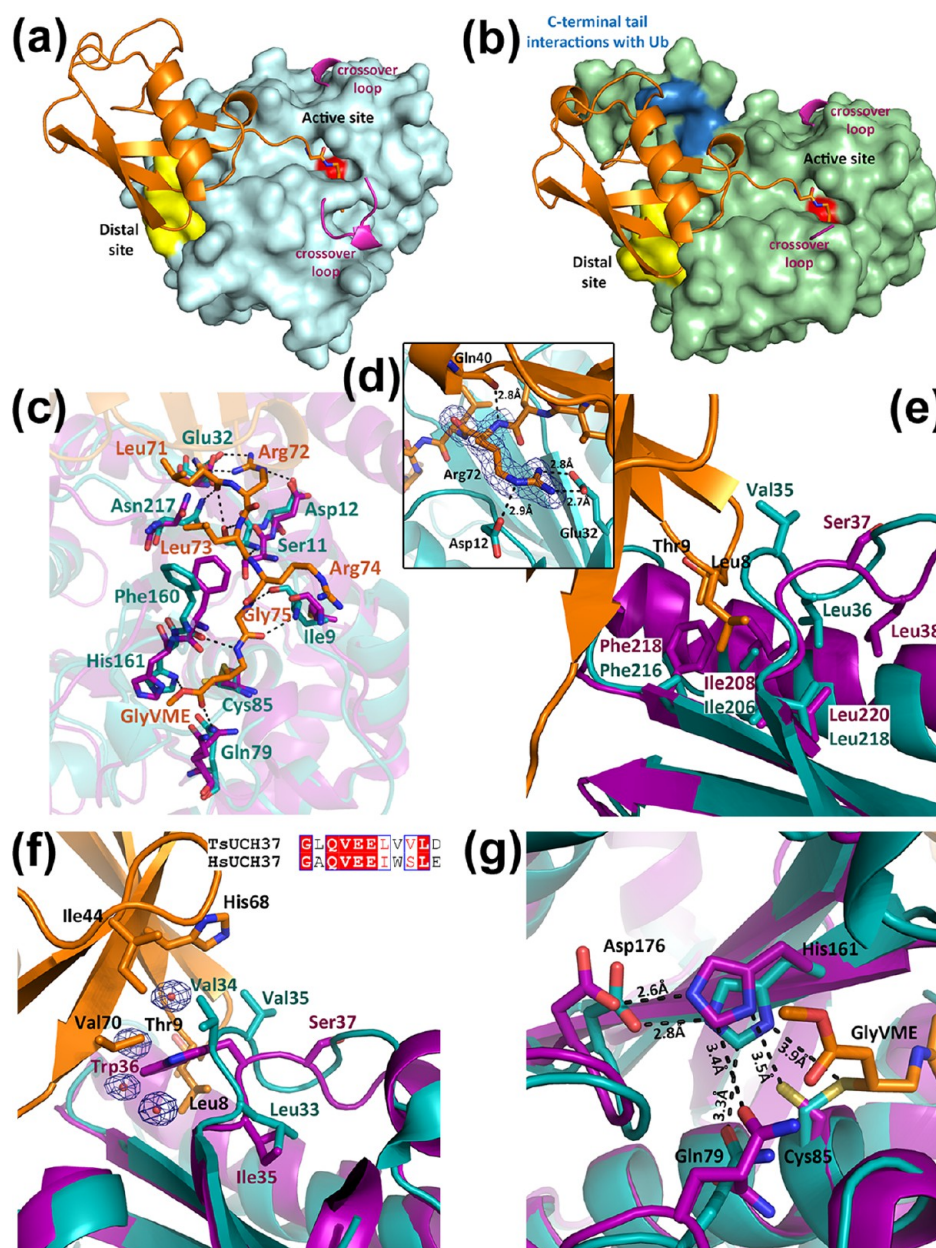


Figure 5. Recognition of ubiquitin by TsUCH37. (a) Surface rendering of TsUCH37^{cat} (cyan) with ubiquitin binding regions highlighted. The distal site is colored yellow and the active-site cysteine red, and resolved portions of the crossover loop are colored pink. (b) Surface rendering of TsUCH37^{ΔC46} (green) with ubiquitin binding regions highlighted as in panel a, except with additional C-terminal tail ubiquitin binding residues colored blue. (c) Interactions near the active-site cleft with the C-terminal hexapeptide tail of ubiquitin. UbVME residues are colored orange, TsUCH37 residues teal, and human UCH37 residues purple. (d) Interactions of Arg72 of ubiquitin with surrounding residues of TsUCH37^{cat}. Density from the 2F_o - F_c map is contoured at 1σ (blue mesh). (e) UCH37 distal-site binding residues, with TsUCH37 colored teal and human UCH37 purple. (f) Ile44 patch interacting residues, with UbVME colored orange, TsUCH37 teal, and human UCH37 purple. Waters involved in binding are also shown, enveloped with density from the 2F_o - F_c map contoured at 1σ. Sequence alignment of this region in TsUCH37 compared to human UCH37 is shown as an inset. (g) Active site of TsUCH37 (teal), showing the catalytic residues, compared to human UCH37 (purple), with UbVME colored orange.

the apo form of either TsUCH37^{cat} or TsUCH37^{ΔC46}. In its place, we use the structure of apo human UCH37 to gain insight into structural changes in the active-site region that may occur upon ubiquitin binding.^{57,58} Comparison with the structures of human UCH37 reveals that the catalytic cysteine has changed its orientation, going from the apo form to the ubiquitin-bound form, adopting a more productive orientation in the latter, an orientation in which the catalytic cysteine's side chain faces the catalytic cleft (Figure 5g). This analysis suggests that UCH37 exists in an unproductive form in the absence of

ubiquitin, with the catalytic thiol facing the interior of the protein rather than the open space in the catalytic cleft,⁵⁸ but is induced to adopt a more productive form upon its binding. Thus, UCH37 may offer yet another example of a UCH DUB that undergoes substrate-induced reorganization to a more productive form.^{48,76}

Crossover Loop Flexibility. A common structural feature present in all UCH enzymes is the crossover loop, which in TsUCH37 spans residues 141–157 (connecting α5 with β3). It straddles the active-site cleft as a flexible loop and is known to

provide steric constraint, limiting the size of the leaving group at the C-terminus of ubiquitin.^{74,77} Accordingly, UCH enzymes, such as UCHL1 and UCHL3, can cleave only small leaving groups from the C-terminus of ubiquitin, not large proteins or another ubiquitin.⁴⁷ However, UCH37 is known to cleave diubiquitin (and polyubiquitin chains), but only when it is associated with the RP, being activated upon binding to its protein cofactor, Rpn13.³⁷ All previously determined structures of UCH enzymes bound to ubiquitin have shown a resolved crossover loop, which makes contact with at least one residue from the C-terminal tail of ubiquitin. In the apo form of UCHL3, the closest homologue of UCH37, the loop is disordered but becomes ordered when ubiquitin is bound.^{48,50} The ubiquitin-bound structures of PfUCHL3 and the yeast ubiquitin hydrolase Yuh1 show an ordered crossover loop making contacts with side chains on the C-terminal tail of ubiquitin.^{73,78} In contrast, the structures of the TsUCH37–UbVME constructs present the only examples so far of a UCH DUB in which the crossover loop is still disordered even after ubiquitin is bound, indicating that the loop is flexible and does not contribute to ubiquitin binding. A small network of van der Waals interactions and hydrogen bonds seem to stabilize part of the crossover loop (residues 152–157) in a short helical conformation in the structure of the TsUCH37^{cat}–UbVME complex, but the same segment in the TsUCH37^{ΔC46}–UbVME structure is disordered and hence not visible, supporting dynamic sampling of conformations by this loop. The observation that the crossover loop is flexible despite the bound ubiquitin may be related to its activation by its proteasome cofactor Rpn13.³⁷ By not engaging with ubiquitin, the loop is available to freely interact with the cofactor, which may stabilize it in a conformation that leaves the active site maximally open to accommodate the isopeptide bond between two ubiquitins or between ubiquitin and an acceptor protein.

Interactions with Ubiquitin. The interaction of UbVME with the TsUCH37^{cat} UCH domain buries a total of 2355 Å² of solvent accessible surface area, a value comparable to the amount buried in other UCH domain ubiquitin complexes (the buried accessible surface area in the TsUCH37^{ΔC46}–UbVME complex is 2479 Å²).^{48,76} The interaction is predominantly localized at two areas on TsUCH37, the active-site cleft and the distal site (Figure 5a,b). The active-site cleft engages the C-terminal hexapeptide segment, Leu⁷¹ArgLeuArgGly-Gly⁷⁶VME, of UbVME with numerous intermolecular contacts that include van der Waals, hydrogen bonding, electrostatic, and water-mediated interactions (Figure 5c). This segment sits in the active-site cleft with an extended conformation to maximize interactions with both backbone and side chain atoms of nearby residues of the enzyme. As seen in other UCH structures, the narrowest part of the active-site cleft surrounds the terminal Gly-Gly motif, with the last Gly (GlyVME in this case) being placed immediately adjacent to the S_Y atom of the catalytic cysteine, precisely located for nucleophilic attack on the scissile peptide bond (Figure 5a,b). It is interesting to note that Arg72 of UbVME is engaged in at least three major interactions (Figure 5d), suggesting that it contributes significantly to stabilizing the enzyme–substrate complex. The interactions with Arg72 imply that TsUCH37 will find NEDD8 (neural precursor cell expressed, developmentally downregulated 8, a structurally similar ubiquitin-like protein modifier with a sequence that is 60% identical with that of ubiquitin) as a poorer substrate because this arginine is replaced with alanine in NEDD8. Indeed, TsUCH37 does not cleave NEDD8-AMC

(see Figure S4 of the Supporting Information). Many of the active-site interactions observed in the ubiquitin-bound structures of UCHL1, UCHL3, PfUCHL3, and Yuh1 are conserved in both TsUCH37 structures. Additionally, those residues surrounding the C-terminal hexapeptide tail of ubiquitin are strongly conserved between the *Ts* and human protein (Figure 5c).

The interactions at the active-site cleft appear to be necessary for precise cleavage at the terminal glycine residue of ubiquitin, while the distal site provides additional interaction to stabilize the enzyme–substrate complex (Figure 5e,f). The distal site engages the N-terminal β -hairpin of ubiquitin, which docks by utilizing interactions primarily involving the two-residue β -turn segment, Leu8 and Thr9 of ubiquitin. These interactions are mostly hydrophobic in nature, involving van der Waals contact of Leu8 and Thr9 with Val35, Leu36, Ile206, Phe216, and Leu218, residues that constitute the surface-exposed hydrophobic crevice that is the distal site. Leu36, Ile206, Phe216, and Leu218 are conserved among *Sp*, *Ts*, *Pf*, and human UCH37 (Figure S3 of the Supporting Information), suggesting the importance of distal-site binding in enzyme–substrate recognition.

Ile44 of ubiquitin, a residue widely used in recognition by ubiquitin-binding proteins, including DUBs, is seen making van der Waals contacts with Val34 on a greasy loop in TsUCH37, residues 34–36 (residues Val35 and Leu36 extend into the distal-site pocket) (Figure 5f). A similar motif is used in other UCH enzymes to bind to Ile44 of ubiquitin. Val34 of TsUCH37 also makes contacts with His68 and Val70, which, together with Ile44 and Leu8 from the N-terminal β -hairpin turn, form the so-called Ile44 patch on ubiquitin. Thus, the binding potential of the Ile44 patch on ubiquitin appears to be fully satisfied in structures of the two complexes presented here, with each residue in the patch making at least one contact with the enzyme. The structural data presented here are supported by previously reported mutational analysis of the PA700 isopeptidase. Replacing Ile44 and Leu8 from the Ile44 patch with alanine in the distal ubiquitin of a diubiquitin substrate results in significantly impaired catalysis with no detectable hydrolysis product.⁴⁵ Val34 and Val35 are replaced with tryptophan and serine, respectively, going from *Ts* to human UCH37 (Figure 5f) (Val34 provides additional contacts with Val70 of UbVME). These residues also show variability among other UCH family members. Subtle differences in the Ile44 patch-binding residues could be one of the contributing factors in the difference in K_M between human and *Ts* UCH37, especially as most of the residues at the active site are conserved between the two.

There appear to be no striking conformational changes between the ubiquitin-bound form of TsUCH37 and apo hUCH37 except for the aforementioned reorientation of the catalytic cysteine. However, we cannot rule out the possibility that significant conformational changes might have occurred as a result of ubiquitin binding in the *Ts* enzyme because we could not crystallize its apo form.

Ubiquitin Binding by the ULD. As mentioned earlier, the ULD of hUCH37 was thought to have an inhibitory role, presumably by folding onto the catalytic domain and obstructing substrate binding.³⁷ In contrast, the structure of the TsUCH37^{ΔC46}–UbVME complex provides crystallographic evidence that the ULD can actually contribute to ubiquitin binding and therefore can play a productive role in catalysis. Arg261 and Tyr262 on α 8 of the ULD approach ubiquitin to

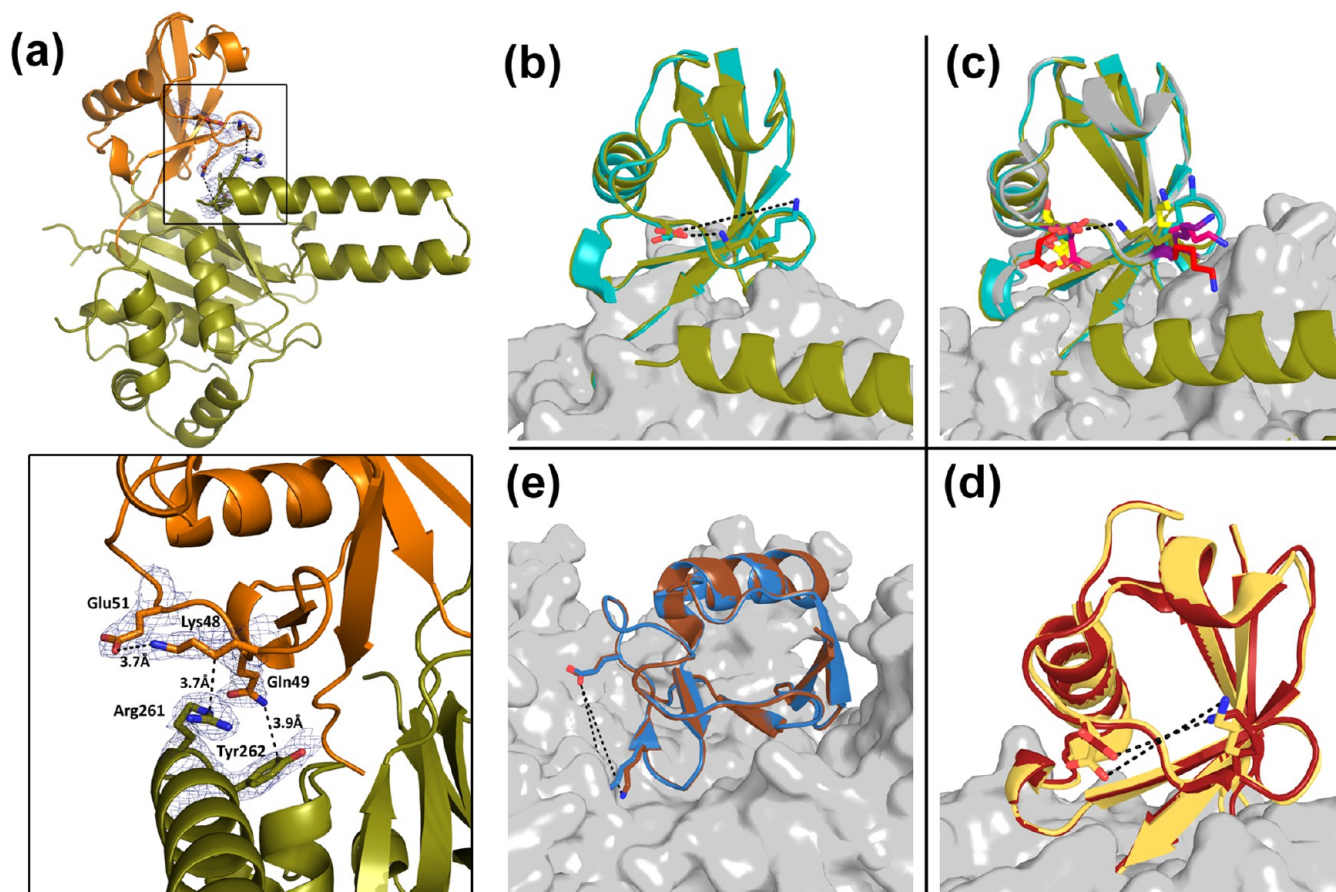


Figure 6. ULD of TsUCH37 binding to ubiquitin. (a) TsUCH37 Δ C46 (olive) ULD residues interacting with UbVME (orange). The inset shows interactions of Arg261 and Tyr262 with UbVME, as well as the intramolecular salt bridge formed between Lys48 and Glu51 of ubiquitin. Density rendered from the $2F_o - F_c$ map contoured to 0.7σ . (b–e) Comparison of the Lys48–Glu51 distances in ubiquitin observed in other DUB–ubiquitin structures. (b) Lys48 and Glu51 form a 3.7 Å salt bridge in the TsUCH37 Δ C46–UbVME structure (olive), but not in the TsUCH37^{cat}–UbVME structure (9.9 Å). (c) The same distance in all other UCH–ubiquitin structures is ≥ 9 Å: UCHL3–UbVME (yellow, PDB entry 1XD3), UCHL1–UbVME (red, PDB entry 3KW5), Yuh1–Ubal (pink, PDB entry 1CMX), PfUCHL3–UbVME (purple, PDB entry 2WDT), and TsUCH37^{cat}–UbVME (teal). (d) The same distance is 8.7 Å in the Otu1–ubiquitin structure (dark red, PDB entry 3BY4) and 6.0 Å in the DUBA–Ubal structure (pale yellow, PDB entry 3TMP). (e) The same distance is 10 Å in the HAUSP/USP7–Ubal structure (blue, PDB entry 1NBF) and 10.9 Å in the USP14–Ubal structure (brown, PDB entry 2AYO).

engage in van der Waals contact with of three of its side chains, Lys48 (with Arg261) and Gln49 and Arg72 (both with Tyr262) (Figure 6). Most notably, Arg261 is oriented in such a way to engage in close van der Waals contact with the hydrocarbon portion of the Lys48 side chain, forcing it to adopt an unusual conformation that allows an intramolecular salt bridge interaction with Glu51. This interaction is not observed in any of the 39 other ubiquitin-bound DUB structures currently found in the PDB, catalogued in Table 3; the Lys48–Glu51 distance is greater than 5.8 Å in all. Figure 6b shows the orientation of the same lysine in the TsUCH37^{cat}–UbVME complex. Clearly, the orientation is different in this structure, and the intramolecular salt bridge in ubiquitin is absent, suggesting that Arg261 of the ULD plays a role in inducing the unusual orientation of Lys48 of ubiquitin. Arg261 is conserved among *Sp*, *Ts*, and human UCH37 (Figure 7) but is replaced with leucine in PfUCH37 (also known as PfUCH54). Tyr262 is conserved in human and *Ts* forms but is substituted with tryptophan in *Sp* and PfUCH37. Inspection of the structure reveals that the van der Waals contact with Lys48 is still feasible with leucine in place of arginine and tryptophan can conservatively replace tyrosine as well. Thus, it is likely that

ULD binding with Lys48 and subsequent formation of the intramolecular salt bridge we are observing here are conserved features of UCH37 in general.

UCH37, as a part of PA700, is known to selectively cleave polyubiquitin chains from the very distal end, sequentially removing one ubiquitin at a time.³⁸ The structural basis of this exo cleavage specificity is not yet known. The unique orientation of Lys48 stabilized by Arg261 leading to the intramolecular salt bridge may explain this selectivity. We propose that although a similar type of interaction between Arg261 and ubiquitin's Lys48 is possible with an internal ubiquitin, the intramolecular salt bridge will be absent in this case because the amino group of the lysine is acylated and hence not charged. Thus, it is the lack of an additional interaction with an internal ubiquitin that makes binding to Lys48 of the terminal ubiquitin more favored, hence the exo selectivity.

DISCUSSION

UCH37 is a proteasome-associated UCH DUB known to have polyubiquitin chain-editing function. It preferentially cleaves the chain from its very distal tip.³⁸ Such a function might rescue

Table 3. Lys48–Glu51 Distances for All DUB–Ubiquitin Complexes

PDB entry	DUB–ubiquitin complex	Lys48–Glu51 distance ^a (Å)
UCH Family		
1XD3	UCHL3–UbVME	9.1, 11.5
1CMX	YUH1–Ubal	10.8
2WDT	PfUCHL3–UbVME	7.3, 9.6
3IFW	UCHL1 S18Y–UbVME	8.7
3KVF	UCHL1 I93M–UbVME	12.3
3KW5	UCHL1–UbVME	13.1
USP Family		
3TMP	DUBA–Ubal	8.3
2YSB	USP21–linear diUbal	7.8, 10.8, 6.6
1NBF	HAUSP–Ubal	10.0, 10.7
2AYO	USP14–Ubal	10.9
3MHS	SAGA complex (UBP8)–Ubal	9.2
2HDS	USP2, Ub	9.0
2G4S	IsoT, Ub	8.6, 8.9
2J7Q	M48 USP–UbVME	9.9, 10.8
3V6E	USP2, Ub variant	7.0
3V6C	USP2, Ub variant	7.4
3IHP	USP5, Ub covalent	9.6, 6.3
3MTN	USP21, ubiquitin-based USP21-specific inhibitor	8.5
3IT3	USP21, Ub covalent	7.4, 7.5, 7.4, 7.4
3N3K	USP8, covalent Ub-like variant	10.4
3NHE	USP2a, Ub	7.4
2IBI	USP2, Ub covalent	7.6
OTU Family		
4IUM	arterivirus papain-like protease 2, Ub	7.4
3ZNH	CCHF viral, Ub-propargyl	9.5
4I6L	OTUB1, Ub	9.1
3PT2	viral OTU, Ub	10.7
4HXD	Nairovirus viral OTU, Ub	8.3, 10.1
3BY4	OTU, Ub	6.0
3PRM	CCHF viral OTU, Ub	9.5, 10.0
3PRP	CCHF viral OTU, Ub	10.3, 10.9
3COR	OTU, Ub	8.4
4DHZ	h/ceOTUB1-ubiquitin aldehyde-UBC13~Ub	9.2, 8.8
4DHJ	ceOTUB1 ubiquitin aldehyde-UBC13~Ub complex	11.4, 8.5, 6.9, 11.8, 9.8, 10.1
4DDI	OTUB1/UbcH5b~Ub/Ub	7.5, 12.6, 12.6, 7.5, 12.6, 7.5
4DDG	OTUB1/UbcH5b~Ub/Ub	11.3, 7.1, 8.0
3PHW	OTU domain of CCHF virus, Ub	7.6, 7.2, 9.0, 5.8
MJD Family		
3O6S	Ataxin-3-like, Ub	9.6, 11.4, 12.8, 11.5
2JRI	Ataxin 3, Ub	12.3, 12.9
JAMM Family		
2ZNV	AMSH-LP, Lys63-linked diubiquitin	9.0, 8.3, 11.9, 11.3

^aMultiple distance entries refer to those in the other subunits of the crystallographic asymmetric unit.

certain substrates from being committed to further downstream action of the proteasome.³⁸ It is also possible that certain substrates carry inappropriate polyubiquitin tags that are not optimal for their degradation. The chain-editing function might be essential for releasing these substrates to clear up ubiquitin receptors for binding to productive substrates. A regulator of proteasome function, it is itself regulated by binding to the proteasome: UCH37 is activated upon binding to Rpn13, a subunit of PA700 (the 19S proteasome or RP), the mechanism

of which is not understood. We report here the structure of two constructs of UCH37 from the infectious helminth *T. spiralis* (*Ts*) bound to the suicide inhibitor UbVME. This work constitutes the first structural analysis of a ubiquitin pathway protein in the organism showing how ubiquitin is recognized by this UCH family DUB in *Ts*. The structures reveal striking conservation of the ubiquitin binding mode among UCH DUBs, from lower eukaryotes to human (Figure S5 of the Supporting Information). It also shows important structural differences between other UCH DUBs, such as UCHL1 and UCHL3, some of which could be used for the specialized function of UCH37. While revealing interesting differences, the *Ts* structures provide a number of details that may also hold true for the human enzyme, advancing our understanding of UCH37 in general.

The active-site cysteine may undergo ubiquitin-mediated reorientation to a more productive form (Figure Sg), making UCH37 yet another example of a UCH DUB that shows regulation of activity by ubiquitin, a feature that may provide selectivity to this group of cysteine proteases. Structures of the two constructs reveal invariant parts of the enzyme, likely less dynamic parts, while also revealing parts that are more dynamic in nature, such as the segment of residues 57–71 and Trp55. Future studies should reveal the role of such dynamic parts in catalysis or regulation thereof.

Importantly, the structure of the construct with the additional 40 amino acids after the UCH domain reveals that the ULD could contribute to ubiquitin binding (Figures 4 and 6), an unexpected finding because it was thought to be inhibitory in the human enzyme.³⁷ The interaction of Arg261 on the ULD appears to engage Lys48 of the distal ubiquitin in a way that would be energetically most favored with the very terminal ubiquitin in a polyubiquitin chain, possibly explaining the exo specificity displayed by mammalian UCH37. These structural data are consistent with previously reported mutational analysis probing substrate specificity of the PA700 isopeptidase: mutation of Lys48 to cysteine on the distal ubiquitin of a diubiquitin substrate results in severely impaired catalysis.⁴⁵ Apart from the broad agreement with the aforementioned experimental work, this observation of the intramolecular Lys48–Glu51 salt bridge in the distal ubiquitin, apparently induced by Arg261, is purely crystallographic at this point, although it seems unlikely that lattice forces have anything to do with it. Even if the opposite is true, the fact that such interactions are physiologically relevant cannot be ignored. The lack of an intramolecular Lys48–Glu51 salt bridge in any other ubiquitin-bound DUB structures to date (Table 3) makes this unusual interaction more intriguing, and worth additional study. This observation therefore lays the structural groundwork for future mutational analysis aimed at validating their existence in solution and their role in substrate specificity.

It is interesting to note that a salt bridge interaction, albeit an intermolecular one, involving Lys48 of ubiquitin and an acidic side chain of the enzyme is also seen in the structure of USP7 bound to ubiquitin aldehyde (the Lys48 side chain of the distal ubiquitin is interacting with Asp305 and Glu308 of USP7).⁷⁹ Such bifurcated salt bridges will perhaps contribute substantially to the binding of the enzyme to distal ubiquitin in a K48-linked chain, based on which one may predict that USP7 will also exhibit exo specificity. This needs to be examined. Preferential cleavage from the very distal tip of a Lys48-linked polyubiquitin chain may be a feature common to DUBs that work on chains of this topology. Lys48-linked chains are known

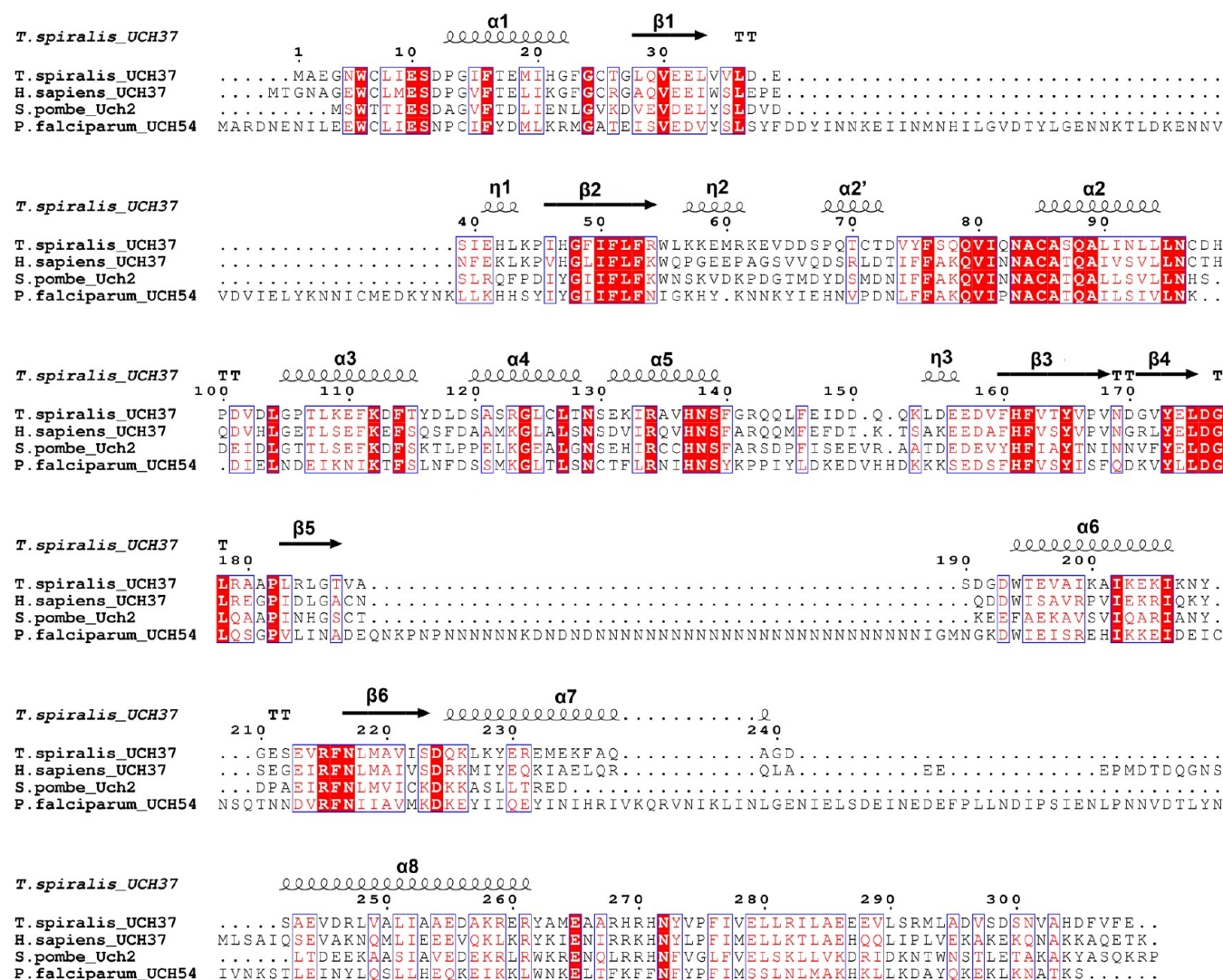


Figure 7. Sequence alignment of TsUCH37 and other homologues: human UCH37, *S. pombe* Uch2, and *Plasmodium falciparum* UCH54. Secondary structures for the two TsUCH37 structures are annotated above (e.g., $\alpha 1$, α -helix 1; $\beta 1$, β -sheet 1; $\eta 1$, 3_{10} -helix 1). $\alpha 2'$ and $\eta 2$ are not resolved in the TsUCH37^{AC46}–UbVME structure, and helices $\alpha 7$ and $\alpha 8$ are not present in the TsUCH37^{cat}–UbVME construct.

to adopt a compact structure.⁸⁰ However, the terminal ubiquitin, being less packed than the internal ones (packed from both sides), is more likely to fray and be susceptible to DUB cleavage for stereochemical reasons. Certain DUBs may have evolved a mechanism for grabbing onto those fraying ends and start disassembling chains from there. There may be other DUBs that prefer internal ubiquitins, or the terminal ones on the other extreme end of the chain, such as isopeptidase-T (USP5),⁸¹ and there may be some with no preference at all. The structure of AMSH-LP (a Lys63-linked chain-specific DUB) in complex with Lys63-linked diubiquitin shows that Lys63 on the distal ubiquitin is not engaged by the enzyme, suggesting it is unlikely to show any preference between the terminal and internal cleavage sites.⁸² This is consistent with the structure of a Lys63-linked chain, which adopts a more extended conformation in crystals and perhaps in solution as well.^{83–85} Future structural studies should reveal more details explaining exo and endo specificity seen in certain DUBs.

The structural analysis, combined with MD simulation, shows the contribution of the ULD in ubiquitin binding. In theory, certain residues in TsUCH37's ULD, missing in our structure, also appear to be correctly positioned for contacting

ubiquitin. Notably, the modeling study provides a possible explanation of why Glu265 and Asn272 are so strictly conserved in UCH37 from different organisms, with virtually no exception. Contributing to ubiquitin binding, as suggested by our modeling studies, may be one of the functional constraints underlying the conservation of the amino acids, although one cannot rule out whether binding to other proteins such as Rpn13 may be involved. It should be noted that Bap1, a UCH DUB mutated in several cancers, also features a ULD.^{70,71,86} Like UCH37, Bap1 becomes activated upon binding to a larger protein complex, demonstrated with the *Drosophila* orthologue, Calypso, binding to the polycomb repressor DUB complex.⁸⁷ Interestingly, the putative ubiquitin-binding residues of the ULD of UCH37 are also conserved in Bap1 (data not shown), suggesting a role in ubiquitin binding for Bap1's ULD as well (in some Bap1 orthologues, the glutamate corresponding to TsUCH37's Glu265 is replaced with an aspartate). However, human Bap1 has a linker of approximately 300 amino acids separating the UCH domain and its ULD. It will be interesting to see how the ULD positions itself to bind ubiquitin, if it does. Of more interest is

knowing whether the ULD has independent ability to bind to ubiquitin.

■ ASSOCIATED CONTENT

■ Supporting Information

Supporting figures and NEDD8 hydrolysis data (Figure S4). This material is available free of charge via the Internet at <http://pubs.acs.org>.

■ Accession Codes

Coordinates and structure factors have been deposited in the Protein Data Bank as entries 4I6N and 4IG7.

■ AUTHOR INFORMATION

■ Corresponding Author

*Brown Laboratory of Chemistry, 560 Oval Dr., West Lafayette, IN 47907. E-mail: cdas@purdue.edu. Phone: (765) 494-5478. Fax: (765) 494-0239.

■ Author Contributions

M.E.M. and M.-I.K. contributed equally to this work.

■ Funding

Financial support from the National Institutes of Health (1R01RR026273, C.D.) is gratefully acknowledged. The General Medicine and Cancer Institutes Collaborative Access Team (GM/CA CAT) of the Advanced Photon Source at Argonne National Laboratory has been funded in whole or in part with Federal funds from the National Cancer Institute (Y1-CO-1020) and the National Institute of General Medical Sciences (Y1-GM-1104).

■ Notes

The authors declare no competing financial interest.

■ ACKNOWLEDGMENTS

We acknowledge Venugopalan Nagarajan, Ruslan Sanishvili, and Craig Ogata at beamline 23-ID-B of the Advanced Photon Source for assistance with data collection. Use of the Advanced Photon Source was supported by the U.S. Department of Energy, Basic Energy Sciences, Office of Science, under Contract DE-AC02-06CH11357. We thank Emma DeWalt and Garth Simpson from the Department of Chemistry, Purdue University, for their assistance with SONICC imaging of initial crystals.

■ ABBREVIATIONS

SDS—PAGE, sodium dodecyl sulfate—polyacrylamide gel electrophoresis; DTT, dithiothreitol; IPTG, isopropyl β -D-1-thiogalactopyranoside; UbVME, ubiquitin vinyl methyl ester; UbAMC, ubiquitin aminomethylcoumarin; UCH37, ubiquitin carboxyl-terminal hydrolase 37; DUB, deubiquitinating enzyme or deubiquitinase; PDB, Protein Data Bank.

■ REFERENCES

- (1) Ciechanover, A. (2005) Proteolysis: From the lysosome to ubiquitin and the proteasome. *Nat. Rev. Mol. Cell Biol.* 6, 79–87.
- (2) Ciechanover, A., and Schwartz, A. L. (2002) Ubiquitin-mediated degradation of cellular proteins in health and disease. *Hepatology* 35, 3–6.
- (3) Varshavsky, A. (1997) The ubiquitin system. *Trends Biochem. Sci.* 22, 383–387.
- (4) Wilkinson, K. D. (2000) Ubiquitination and deubiquitination: Targeting of proteins for degradation by the proteasome. *Semin. Cell Dev. Biol.* 11, 141–148.
- (5) Goldberg, A. L. (2003) Protein degradation and protection against misfolded or damaged proteins. *Nature* 426, 895–899.

- (6) Pickart, C. M., and Cohen, R. E. (2004) Proteasomes and their kin: Proteases in the machine age. *Nat. Rev. Mol. Cell Biol.* 5, 177–187.
- (7) Finley, D. (2009) Recognition and processing of ubiquitin-protein conjugates by the proteasome. *Annu. Rev. Biochem.* 78, 477–513.
- (8) Baumeister, W., Walz, J., Zuhl, F., and Seemuller, E. (1998) The proteasome: Paradigm of a self-compartmentalizing protease. *Cell* 92, 367–380.
- (9) Matyskiela, M. E., and Martin, A. (2012) Design principles of a universal protein degradation machine. *J. Mol. Biol.* 425, 199–213.
- (10) Lander, G. C., Estrin, E., Matyskiela, M. E., Bashore, C., Nogales, E., and Martin, A. (2012) Complete subunit architecture of the proteasome regulatory particle. *Nature* 482, 186–191.
- (11) Lasker, K., Forster, F., Bohn, S., Walzthoeni, T., Villa, E., Unverdorben, P., Beck, F., Aebersold, R., Sali, A., and Baumeister, W. (2012) Molecular architecture of the 26S proteasome holocomplex determined by an integrative approach. *Proc. Natl. Acad. Sci. U.S.A.* 109, 1380–1387.
- (12) Goldberg, A. L. (2007) Functions of the proteasome: From protein degradation and immune surveillance to cancer therapy. *Biochem. Soc. Trans.* 35, 12–17.
- (13) Demartino, G. N., and Gillette, T. G. (2007) Proteasomes: Machines for all reasons. *Cell* 129, 659–662.
- (14) Guterman, A., and Glickman, M. H. (2004) Deubiquitinating enzymes are IN/(trinsic to proteasome function). *Curr. Protein Pept. Sci.* 5, 201–211.
- (15) Yao, T., and Cohen, R. E. (2002) A cryptic protease couples deubiquitination and degradation by the proteasome. *Nature* 419, 403–407.
- (16) Verma, R., Aravind, L., Oania, R., McDonald, W. H., Yates, J. R., III, Koonin, E. V., and Deshaies, R. J. (2002) Role of Rpn11 metalloprotease in deubiquitination and degradation by the 26S proteasome. *Science* 298, 611–615.
- (17) Lee, M. J., Lee, B. H., Hanna, J., King, R. W., and Finley, D. (2011) Trimming of ubiquitin chains by proteasome-associated deubiquitinating enzymes. *Mol. Cell Proteomics* 10, R110.003871.
- (18) Pickart, C. M. (2001) Mechanisms underlying ubiquitination. *Annu. Rev. Biochem.* 70, 503–533.
- (19) Schulman, B. A. (2011) Twists and turns in ubiquitin-like protein conjugation cascades. *Protein Sci.* 20, 1941–1954.
- (20) Pickart, C. M. (2000) Ubiquitin in chains. *Trends Biochem. Sci.* 25, 544–548.
- (21) Haglund, K., and Dikic, I. (2005) Ubiquitylation and cell signaling. *EMBO J.* 24, 3353–3359.
- (22) Ikeda, F., and Dikic, I. (2008) Atypical ubiquitin chains: New molecular signals. 'Protein Modifications: Beyond the Usual Suspects' review series. *EMBO Rep.* 9, 536–542.
- (23) Fushman, D., and Wilkinson, K. D. (2011) Structure and recognition of polyubiquitin chains of different lengths and linkage. *F1000 Biol. Rep.* 3, 26.
- (24) Komander, D., and Rape, M. (2012) The ubiquitin code. *Annu. Rev. Biochem.* 81, 203–229.
- (25) Kulathu, Y., and Komander, D. (2012) Atypical ubiquitylation: The unexplored world of polyubiquitin beyond Lys48 and Lys63 linkages. *Nat. Rev. Mol. Cell Biol.* 13, 508–523.
- (26) Chen, Z. J., and Sun, L. J. (2009) Nonproteolytic functions of ubiquitin in cell signaling. *Mol. Cell* 33, 275–286.
- (27) Komander, D., Clague, M. J., and Urbe, S. (2009) Breaking the chains: Structure and function of the deubiquitinases. *Nat. Rev. Mol. Cell Biol.* 10, 550–563.
- (28) Komander, D. (2010) Mechanism, specificity and structure of the deubiquitinases. *Subcell. Biochem.* 54, 69–87.
- (29) Amerik, A. Y., and Hochstrasser, M. (2004) Mechanism and function of deubiquitinating enzymes. *Biochim. Biophys. Acta* 1695, 189–207.
- (30) Wilkinson, K. D. (1997) Regulation of ubiquitin-dependent processes by deubiquitinating enzymes. *FASEB J.* 11, 1245–1256.
- (31) Wilkinson, K. D. (2009) DUBs at a glance. *J. Cell Sci.* 122, 2325–2329.

- (32) Nijman, S. M., Luna-Vargas, M. P., Velds, A., Brummelkamp, T. R., Dirac, A. M., Sixma, T. K., and Bernards, R. (2005) A genomic and functional inventory of deubiquitinating enzymes. *Cell* 123, 773–786.
- (33) Love, K. R., Catic, A., Schlieker, C., and Ploegh, H. L. (2007) Mechanisms, biology and inhibitors of deubiquitinating enzymes. *Nat. Chem. Biol.* 3, 697–705.
- (34) Reyes-Turcu, F. E., Ventii, K. H., and Wilkinson, K. D. (2009) Regulation and cellular roles of ubiquitin-specific deubiquitinating enzymes. *Annu. Rev. Biochem.* 78, 363–397.
- (35) Tsou, W. L., Sheedlo, M. J., Morrow, M. E., Blount, J. R., McGregor, K. M., Das, C., and Todi, S. V. (2012) Systematic analysis of the physiological importance of deubiquitinating enzymes. *PLoS One* 7, e43112.
- (36) Borodovsky, A., Kessler, B. M., Casagrande, R., Overkleeft, H. S., Wilkinson, K. D., and Ploegh, H. L. (2001) A novel active site-directed probe specific for deubiquitylating enzymes reveals proteasome association of USP14. *EMBO J.* 20, 5187–5196.
- (37) Yao, T., Song, L., Xu, W., DeMartino, G. N., Florens, L., Swanson, S. K., Washburn, M. P., Conaway, R. C., Conaway, J. W., and Cohen, R. E. (2006) Proteasome recruitment and activation of the Uch37 deubiquitinating enzyme by Adrm1. *Nat. Cell Biol.* 8, 994–1002.
- (38) Lam, Y. A., Xu, W., DeMartino, G. N., and Cohen, R. E. (1997) Editing of ubiquitin conjugates by an isopeptidase in the 26S proteasome. *Nature* 385, 737–740.
- (39) Hanna, J., Hathaway, N. A., Tone, Y., Crosas, B., Elsasser, S., Kirkpatrick, D. S., Leggett, D. S., Gygi, S. P., King, R. W., and Finley, D. (2006) Deubiquitinating enzyme Ubp6 functions noncatalytically to delay proteasomal degradation. *Cell* 127, 99–111.
- (40) Hu, M., Li, P., Song, L., Jeffrey, P. D., Chenova, T. A., Wilkinson, K. D., Cohen, R. E., and Shi, Y. (2005) Structure and mechanisms of the proteasome-associated deubiquitinating enzyme USP14. *EMBO J.* 24, 3747–3756.
- (41) Koulich, E., Li, X., and DeMartino, G. N. (2008) Relative structural and functional roles of multiple deubiquitylating proteins associated with mammalian 26S proteasome. *Mol. Biol. Cell* 19, 1072–1082.
- (42) Lee, B. H., Lee, M. J., Park, S., Oh, D. C., Elsasser, S., Chen, P. C., Gartner, C., Dimova, N., Hanna, J., Gygi, S. P., Wilson, S. M., King, R. W., and Finley, D. (2010) Enhancement of proteasome activity by a small-molecule inhibitor of USP14. *Nature* 467, 179–184.
- (43) D'Arcy, P., Brnjic, S., Olofsson, M. H., Fryknaas, M., Lindsten, K., De Cesare, M., Perego, P., Sadeghi, B., Hassan, M., Larsson, R., and Linder, S. (2011) Inhibition of proteasome deubiquitinating activity as a new cancer therapy. *Nat. Med.* 17, 1636–1640.
- (44) D'Arcy, P., and Linder, S. (2012) Proteasome deubiquitinases as novel targets for cancer therapy. *Int. J. Biochem. Cell Biol.* 44, 1729–1738.
- (45) Lam, Y. A., DeMartino, G. N., Pickart, C. M., and Cohen, R. E. (1997) Specificity of the ubiquitin isopeptidase in the PA700 regulatory complex of 26 S proteasomes. *J. Biol. Chem.* 272, 28438–28446.
- (46) Stone, M., Hartmann-Petersen, R., Seeger, M., Bech-Otschir, D., Wallace, M., and Gordon, C. (2004) Uch2/Uch37 is the major deubiquitinating enzyme associated with the 26S proteasome in fission yeast. *J. Mol. Biol.* 344, 697–706.
- (47) Larsen, C. N., Krantz, B. A., and Wilkinson, K. D. (1998) Substrate specificity of deubiquitinating enzymes: Ubiquitin C-terminal hydrolases. *Biochemistry* 37, 3358–3368.
- (48) Misaghi, S., Galaray, P. J., Meester, W. J., Ovaa, H., Ploegh, H. L., and Gaudet, R. (2005) Structure of the ubiquitin hydrolase UCH-L3 complexed with a suicide substrate. *J. Biol. Chem.* 280, 1512–1520.
- (49) Das, C., Hoang, Q. Q., Kreinbring, C. A., Luchansky, S. J., Meray, R. K., Ray, S. S., Lansbury, P. T., Ringe, D., and Petsko, G. A. (2006) Structural basis for conformational plasticity of the Parkinson's disease-associated ubiquitin hydrolase UCH-L1. *Proc. Natl. Acad. Sci. U.S.A.* 103, 4675–4680.
- (50) Johnston, S. C., Larsen, C. N., Cook, W. J., Wilkinson, K. D., and Hill, C. P. (1997) Crystal structure of a deubiquitinating enzyme (human UCH-L3) at 1.8 Å resolution. *EMBO J.* 16, 3787–3796.
- (51) Hamazaki, J., Iemura, S., Natsume, T., Yashiroda, H., Tanaka, K., and Murata, S. (2006) A novel proteasome interacting protein recruits the deubiquitinating enzyme UCH37 to 26S proteasomes. *EMBO J.* 25, 4524–4536.
- (52) Husnjak, K., Elsasser, S., Zhang, N., Chen, X., Randles, L., Shi, Y., Hofmann, K., Walters, K. J., Finley, D., and Dikic, I. (2008) Proteasome subunit Rpn13 is a novel ubiquitin receptor. *Nature* 453, 481–488.
- (53) Schreiner, P., Chen, X., Husnjak, K., Randles, L., Zhang, N., Elsasser, S., Finley, D., Dikic, I., Walters, K. J., and Groll, M. (2008) Ubiquitin docking at the proteasome through a novel pleckstrin-homology domain interaction. *Nature* 453, 548–552.
- (54) Qiu, X. B., Ouyang, S. Y., Li, C. J., Miao, S., Wang, L., and Goldberg, A. L. (2006) hRpn13/ADRM1/GP110 is a novel proteasome subunit that binds the deubiquitinating enzyme, UCH37. *EMBO J.* 25, 5742–5753.
- (55) Yao, T., Song, L., Jin, J., Cai, Y., Takahashi, H., Swanson, S. K., Washburn, M. P., Florens, L., Conaway, R. C., Cohen, R. E., and Conaway, J. W. (2008) Distinct modes of regulation of the Uch37 deubiquitinating enzyme in the proteasome and in the Ino80 chromatin-remodeling complex. *Mol. Cell* 31, 909–917.
- (56) Nishio, K., Kim, S. W., Kawai, K., Mizushima, T., Yamane, T., Hamazaki, J., Murata, S., Tanaka, K., and Morimoto, Y. (2009) Crystal structure of the de-ubiquitinating enzyme UCH37 (human UCH-L5) catalytic domain. *Biochem. Biophys. Res. Commun.* 390, 855–860.
- (57) Burgie, S. E., Bingman, C. A., Soni, A. B., and Phillips, G. N. (2012) Structural characterization of human Uch37. *Proteins* 80, 649–654.
- (58) Maiti, T. K., Permaul, M., Boudreaux, D. A., Mahanic, C., Mauney, S., and Das, C. (2011) Crystal structure of the catalytic domain of UCHL5, a proteasome-associated human deubiquitinating enzyme, reveals an unproductive form of the enzyme. *FEBS J.* 278, 4917–4926.
- (59) White, R. R., Miyata, S., Papa, E., Spooner, E., Gounaris, K., Selkirk, M. E., and Artavanis-Tsakonas, K. (2011) Characterisation of the *Trichinella spiralis* deubiquitinating enzyme, TsUCH37, an evolutionarily conserved proteasome interaction partner. *PLoS Neglected Trop. Dis.* 5, e1340.
- (60) Borodovsky, A., Ovaa, H., Kolli, N., Gan-Erdene, T., Wilkinson, K. D., Ploegh, H. L., and Kessler, B. M. (2002) Chemistry-based functional proteomics reveals novel members of the deubiquitinating enzyme family. *Chem. Biol.* 9, 1149–1159.
- (61) Holyoak, T., Fenn, T. D., Wilson, M. A., Moulin, A. G., Ringe, D., and Petsko, G. A. (2003) Malonate: A versatile cryoprotectant and stabilizing solution for salt-grown macromolecular crystals. *Acta Crystallogr. D* 59, 2356–2358.
- (62) Otwinowski, Z., and Minor, W. (1997) Processing of X-ray Diffraction Data Collected in Oscillation Mode. *Methods Enzymol.* 276, 307–326.
- (63) Adams, P. D., Afonine, P. V., Bunkoczi, G., Chen, V. B., Davis, I. W., Echols, N., Headd, J. J., Hung, L.-W., Kapral, G. J., and Grosse-Kunstleve, R. W. (2010) PHENIX: A comprehensive Python-based system for macromolecular structure solution. *Acta Crystallogr. D* 66, 213–221.
- (64) Emsley, P., and Cowtan, K. (2004) Coot: Model-building tools for molecular graphics. *Acta Crystallogr. D* 60, 2126–2132.
- (65) Schuck, P. (2000) Size-distribution analysis of macromolecules by sedimentation velocity ultracentrifugation and lamm equation modeling. *Biophys. J.* 78, 1606–1619.
- (66) Arnold, K., Bordoli, L., Kopp, J., and Schwede, T. (2006) The SWISS-MODEL workspace: A web-based environment for protein structure homology modelling. *Bioinformatics* 22, 195–201.
- (67) Case, D., Darden, T., Cheatham, T., III, Simmerling, C., Wang, J., Duke, R., Luo, R., Walker, R., Zhang, W., and Merz, K. (2012) AMBER 12, University of California, San Francisco.

- (68) Darden, T., York, D., and Pedersen, L. (1993) Particle mesh Ewald: An N-log (N) method for Ewald sums in large systems. *J. Chem. Phys.* 98, 10089.
- (69) Ryckaert, J.-P., Ciccotti, G., and Berendsen, H. J. (1977) Numerical integration of the cartesian equations of motion of a system with constraints: Molecular dynamics of *n*-alkanes. *J. Comput. Phys.* 23, 327–341.
- (70) Misaghi, S., Ottosen, S., Izrael-Tomasevic, A., Arnott, D., Lamkanfi, M., Lee, J., Liu, J., O'Rourke, K., Dixit, V. M., and Wilson, A. C. (2009) Association of C-terminal ubiquitin hydrolase BRCA1-associated protein 1 with cell cycle regulator host cell factor 1. *Mol. Cell. Biol.* 29, 2181–2192.
- (71) Sanchez-Pulido, L., Kong, L., and Ponting, C. P. (2012) A common ancestry for BAP1 and Uch37 regulators. *Bioinformatics* 28, 1953–1956.
- (72) Chen, V., Arendall, W., Headd, J., Keedy, D., Immormino, R., Kapral, G., Murray, L., Richardson, J., and Richardson, D. (2010) MolProbity: All-atom structure validation for macromolecular crystallography. *Acta Crystallogr. D* 66, 12–21.
- (73) Johnston, S. C., Riddle, S. M., Cohen, R. E., and Hill, C. P. (1999) Structural basis for the specificity of ubiquitin C-terminal hydrolases. *EMBO J.* 18, 3877–3887.
- (74) Zhou, Z. R., Zhang, Y. H., Liu, S., Song, A. X., and Hu, H. Y. (2012) Length of the active-site crossover loop defines the substrate specificity of ubiquitin C-terminal hydrolases for ubiquitin chains. *Biochem. J.* 441, 143–149.
- (75) Boudreaux, D. A., Chaney, J., Maiti, T. K., and Das, C. (2012) Contribution of active site glutamine to rate enhancement in ubiquitin C-terminal hydrolases. *FEBS J.* 279, 1106–1118.
- (76) Boudreaux, D. A., Maiti, T. K., Davies, C. W., and Das, C. (2010) Ubiquitin vinyl methyl ester binding orients the misaligned active site of the ubiquitin hydrolase UCHL1 into productive conformation. *Proc. Natl. Acad. Sci. U.S.A.* 107, 9117–9122.
- (77) Popp, M. W., Artavanis-Tsakonas, K., and Ploegh, H. L. (2009) Substrate filtering by the active site crossover loop in UCHL3 revealed by sortagging and gain-of-function mutations. *J. Biol. Chem.* 284, 3593–3602.
- (78) Artavanis-Tsakonas, K., Weihofen, W. A., Antos, J. M., Coleman, B. I., Comeaux, C. A., Duraisingh, M. T., Gaudet, R., and Ploegh, H. L. (2010) Characterization and structural studies of the *Plasmodium falciparum* ubiquitin and Nedd8 hydrolase UCHL3. *J. Biol. Chem.* 285, 6857–6866.
- (79) Hu, M., Li, P., Li, M., Li, W., Yao, T., Wu, J. W., Gu, W., Cohen, R. E., and Shi, Y. (2002) Crystal structure of a UBP-family deubiquitinating enzyme in isolation and in complex with ubiquitin aldehyde. *Cell* 111, 1041–1054.
- (80) Eddins, M. J., Varadan, R., Fushman, D., Pickart, C. M., and Wolberger, C. (2007) Crystal structure and solution NMR studies of Lys48-linked tetraubiquitin at neutral pH. *J. Mol. Biol.* 367, 204–211.
- (81) Reyes-Turcu, F. E., Shanks, J. R., Komander, D., and Wilkinson, K. D. (2008) Recognition of polyubiquitin isoforms by the multiple ubiquitin binding modules of isopeptidase T. *J. Biol. Chem.* 283, 19581–19592.
- (82) Sato, Y., Yoshikawa, A., Yamagata, A., Mimura, H., Yamashita, M., Ookata, K., Nureki, O., Iwai, K., Komada, M., and Fukai, S. (2008) Structural basis for specific cleavage of Lys 63-linked polyubiquitin chains. *Nature* 455, 358–362.
- (83) Datta, A. B., Hura, G. L., and Wolberger, C. (2009) The structure and conformation of Lys63-linked tetraubiquitin. *J. Mol. Biol.* 392, 1117–1124.
- (84) Komander, D., Reyes-Turcu, F., Licchesi, J. D., Odenwaelde, P., Wilkinson, K. D., and Barford, D. (2009) Molecular discrimination of structurally equivalent Lys 63-linked and linear polyubiquitin chains. *EMBO Rep.* 10, 466–473.
- (85) Tenno, T., Fujiwara, K., Tochio, H., Iwai, K., Morita, E. H., Hayashi, H., Murata, S., Hiroaki, H., Sato, M., Tanaka, K., and Shirakawa, M. (2004) Structural basis for distinct roles of Lys63- and Lys48-linked polyubiquitin chains. *Genes Cells* 9, 865–875.
- (86) Ventii, K. H., Devi, N. S., Friedrich, K. L., Chernova, T. A., Tighiouart, M., Van Meir, E. G., and Wilkinson, K. D. (2008) BRCA1-associated protein-1 is a tumor suppressor that requires deubiquitinating activity and nuclear localization. *Cancer Res.* 68, 6953–6962.
- (87) Scheuermann, J. C., de Ayala Alonso, A. G., Oktaba, K., Ly-Hartig, N., McGinty, R. K., Fraterman, S., Wilm, M., Muir, T. W., and Muller, J. (2010) Histone H2A deubiquitinase activity of the Polycomb repressive complex PR-DUB. *Nature* 465, 243–247.